RSC Advances

ROYAL SOCIETY OF CHEMISTRY

www.rsc.org/advances

RSC Advances

ARTICLE

Alginate fibers embedded with silver nanoparticles as efficient catalysts for reduction of 4-nitrophenol

Received 00th January 20xx,
Accepted 00th January 20xx

DOI: 10.1039/x0xx00000x

www.rsc.org/

X. H. Zhao,[a,c,*] Q. Li,[a,c] X. M. Ma,[a,c] Z. Xiong,[a,c] F. Quan,[a,c] and Y. Z. Xia [b,c,*]

Silver nanoparticles (AgNPs) have attracted much attention as promising catalysts in various electron transfer reactions due to their high catalytic efficiency. However, their poor stability results in the decrease of the catalytic efficiency and the poor cycling performance, which have hindered the practical application of AgNPs. In this work, alginate fibers embedded with AgNPs were prepared *via* in situ reduction of Ag^+-alginate fibers in the presence of glucose. Field emission scanning electron microscopy (FE-SEM) and Transmission electron microscopy (TEM) indicated that spherical AgNPs dispersed on the surface and the interior of the fibers. The alginate fibers could enable AgNPs to be highly stabilized and thus led to the excellent reusability as heterogeneous catalysts for the reduction of 4-nitrophenol (4-NP) to 4-aminophenol (4-AP) in aqueous media. The catalytic results indicated that 4-NP could be reduced completely within 15 min. Moreover, the catalyst was easily recovered and reused for at least ten cycles in the reduction reactions, confirming its excellent stability. Most importantly, compared to the conventional powdery catalysts, the fiber catalyst could be handled much more conveniently for re-usage owing to its easily separation.

1. Introduction

Silver nanoparticles (AgNPs) have attracted tremendous attention in the past few decades due to their unique physical and chemical properties, which give them remarkable potential for applications in catalytic, electronic, optical, biological, and medical fields.[1-3] AgNPs show noticeable reduction potential in comparison to bulk metals as the Fermi potential of nanoparticles becomes more negative. This particular property allows them to act as catalysts in various electron transfer reactions.[4, 5] Unfortunately, AgNPs tend to easily aggregate and change shape during catalytic reactions because of their high surface energy resulting from the high surface-to-volume ratio, and result in a remarkable reduction in their catalytic activity and selectivity undesirably.[6-8] Consequently, it is desirable to explore simple and effective methods to maintain the long-term stability so as to determine the catalytic performance of AgNPs. A classic method is immobilization or encapsulation of AgNPs on/into supporting matrix.[9-12] Hybrid catalysts integrated AgNPs with inorganic and organic supports have been successfully developed.[9, 13-16] Polymer，especially renewable and nonhazardous biopolymer matrix as a support for metal nanocatalysts have attracted considerable attention.[17-21] Lu et al. reported on the in situ synthesis of AgNPs onto polystyrene (PS) core-poly(acrylic acid) (PAA) polyelectrolyte brush particles.[22] Wu et al. prepared cellulose/AgNPs composites with porous cellulose microspheres served as supports for AgNPs.[23] However, these strategies need either complicated synthesis or have relatively high cost. Thus, simple and commercial viability method to prepare hybrid catalysts immobilized AgNPs with supports are still highly desired.

Alginate, isolated from marine algae is a copolymer of β-D-mannuronic acid (M) and α-L-guluronic acid (G). Alginate fiber, as bio-based fiber, could be prepared by dispersing wetspun sodium alginate into a coagulating bath containing $CaCl_2$ aqueous solution.[24] Ca^{2+} cations induce interchain association between long stretches of G units and the formation of the gel junction zones, and the structure has been described by the so-called egg-box model.[25, 26] The obtained alginate fibers were favourable as supporting material to stabilize AgNPs with easily accessible high surface area attributed to the fibers with large length-diameter ratio. Herein, we develop a simple and accessible approach to fabricate AgNPs supported on alginate fibers *via* in situ reduction of Ag^+-alginate fibers. As illustrated in Scheme 1, alginate fibers were initially immersed into an aqueous solution of $AgNO_3$. The Ag^+ ions diffused into the alginate fibers and reacted with the fibers *via* ion-exchange with

[a] College of chemistry and chemical engineering, Qingdao University, Qingdao 266071, P R China. E-mail: gaozxh@163.com; qdxyzh@qdu.edu.cn
[b] State Key Laboratory Cultivating Base for New Fiber Materials and Modern Textiles, Qingdao University, Qingdao 266071,P R China
[c] Collaborative Innovation Center for Marine Biomass Fibers, Materials and Textiles of Shandong Province, Qingdao University, Qingdao 266071, P R China

† Footnotes relating to the title and/or authors should appear here. Electronic Supplementary Information (ESI) available: [details of any supplementary information available should be included here]. See DOI:10.1039/x0xx00000x

calcium ions or sodium ion in the fibers. The negatively charged alginate facilitated the attraction of the positively charged silver ions by electrostatic attraction, resulting in the attachment of Ag^+ to alginate fibers. Then, silver ions were reduced in situ, metallic silver were generated and tended to adhere to the alginate fibers, forming silver seeds. Subsequently, AgNPs were gradually generated and closely deposited on alginate fibers. The resulting alginate-AgNPs fibers were well characterized and their catalytic property was explored as an efficient green catalyst for the reduction of anthropogenic pollutant 4-NP.

4-NP is one of the most common hazardous organic pollutants and contaminates the environment. while, the reduced product, 4-AP is a very important intermediate for the production various analgesic and antipyretic drugs and also has potential applications in dyeing agent, photographic developers, and corrosion inhibitors.[27, 28] Nonetheless, the reduction of 4-NP by traditional methods are mostly ineffective due to the high stability and low solubility of 4-NP in water. Therefore, there is a great demand for the direct catalytic reduction of 4-NP into 4-AP with facile and efficient method. It will be shown later that the as-prepared fibers represent an effective catalyst for 4-NP reduction, moreover, it could enable AgNPs to be highly stabilized and could be handled much more conveniently for re-usage in different runs owing to its monolithic structure compared to the conventional powdery catalysts.

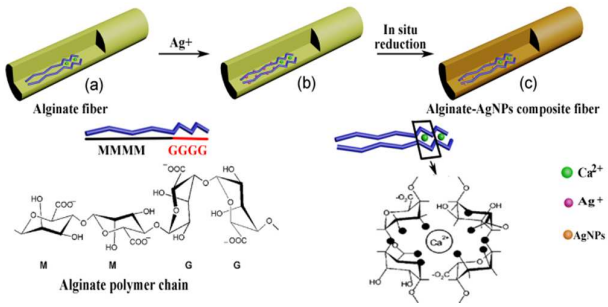

Scheme 1 Schematic representation of the preparation of alginate-AgNPs fibers in situ.

2. Experimental

2.1. Reagents

Sodium alginate (SA) was supplied by Jiejing Seaweed Co. Ltd., Rizhao, Shandong Province, P. R. China. Analytical grade silver nitrate ($AgNO_3$), glucose, methylene blue, 4-nitrophenol (4-NP) and sodium borohydride ($NaBH_4$) were purchased from commercial sources in China and used as supplied. All solutions were prepared with deionized water.

2.2. Preparation of alginate fibers

Alginate fibers were firstly prepared by wet-spinning technique. Briefly, sodium alginate was dissolved in water under stirring to obtain homogenous, well-flowing viscous solution suitable for spinning, and filtered through a 200-mesh filter cloth under pressure. The clear filtrate was degassed in a spinning tank. Then, the spinning solution was extruded through a 30-hole (0.08 mm diameter) stainless steel spinneret by a metering pump into a coagulation bath containing a 5 wt% aqueous calcium chloride. The resulting alginate fibers were stretched (the stretching ratio was 20%), washed with distilled water and dried.

2.3. Preparation of alginate- AgNPs fibers

0.4g of the prepared alginate fibers was immersed in $AgNO_3$ aqueous solutions 24 mL at room temperature for 1 h. After that, 1 mL glucose solution (1 wt%) was added and the mixture was heated at 50-80 ^oC for 45 min in an oscillating water bath. The color of alginate fibers in the solution became yellow or brown. The fibers were taken out and rinsed with deionized water, and then were dried at room temperature. The fibers prepared by this method were named hereafter as alginate-AgNPs fibers.

2.4. Characterization

Silver content of the alginate-AgNPs fibers was determined by Inductively coupled plasma optical emission spectrometry (ICP-OES) (Perkin-Elmer Optima 8000, USA) according to the previous work.[29] For an instrumental calibration (1–0.5–0.1–0.05–0.02 mg/L), a commercially available stock standard solution of Ag containing 1 g/L were used. The limits of detection (the concentration equivalent to three times standard deviation of the blank sample in the place of background correction) were 10 g/L for lines 338.289 nm and 328.068 nm. For analysis of real samples, results from both analytical lines used were average. Field emission scanning electron microscopy (FE-SEM) images were recorded using a JSM-7500F field emission scanning electron microscope equipped with an energy dispersive x-ray spectroscopy (EDS) detector. X-ray diffraction (XRD) measurements of pure alginate fibers and alginate-AgNPs fibers were carried out on a powder X-ray diffractometer (D/MAX-RB) using CuKα radiation (λ= 0.15418 nm) over a 2θ range of 5°-80° with a step size of 0.05°. Transmission electron microscopy (TEM) images were obtained by a JEM-1200EX microscope at an accelerating voltage of 100.0 kV. In the case of the alginate-AgNPs fibers, ultrathin sections of 60 nm thickness were prepared by embedding the fibers into resin and cutting using RMC ultramicrotome, the sections was analyzed using TEM to reveal the distribution of nanoparticles. X-ray photoelectron spectroscopy (XPS) measurement was conducted with ESCALAB 250 spectrometer (ThermoFisher Scientific, USA) with an Al Kα radiation as the X-ray source (hν = 1486.7 eV). The peak positions were corrected for sample charging by setting the C 1s binding energy at 284.8 eV.

2.5 Catalytic reduction of 4-NP

To evaluate the catalytic activity of the alginate-AgNPs fibers, we chose the reduction of 4-NP by $NaBH_4$ as a model reaction. Firstly, freshly prepared 5.0 mL 0.05 M $NaBH_4$ aqueous solution was mixed with 0.5 mL of 1 mM 4-NP aqueous solution in the quartz cell. Then, 5mg of the

synthesized alginate-AgNPs fibers was added into the above solution. The progress of the conversion of 4-NP to 4-AP at ambient temperature was monitored via UV-vis spectrophotometer (Shimadzu UV3150) by scanning a range of 200-550 nm.

3. Results and discussion

3.1. In situ synthesis of alginate- AgNPs fibers

The preparation of alginate-AgNPs fibers followed a simple procedure which was performed in an atmosphere of nitrogen and exclusion of light. Prior to heating, the alginate fibers were soaked in the silver nitrate solution for 1 h. Subsequently, the suspensions were heated to desired temperature (50-80 ^{o}C). Fig. 1(a) shows the photos of pure alginate fibers (colorless) and the alginate-AgNPs fibers prepared at different temperature. The results indicate that AgNPs in situ grow onto the alginate fibers after heating, yielding yellow or brown colored fiber material. The brilliant color of the fibers is from the local surface plasmon resonance of loaded AgNPs. [30] Fig. 1(b) shows the content of silver nanoparticles incorporated into alginate fibers expressed as the percentage per dry fiber weight. It can be seen that the silver percentage in the fibers increase with the increasing of reaction temperature. This might be due to the higher reduction efficiency of Ag^{+} to AgNPs at higher temperature.

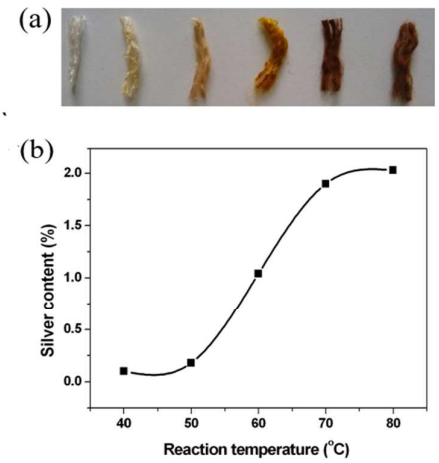

Fig. 1 (a) Photos of pure alginate fibers and alginate-AgNPs fibers: from left-hand side to right hand side: pure alginate fibers, alginate-AgNPs fibers synthesized at 40, 50, 60, 70 and 80 °C, $AgNO_3$ 12 mM, respectively. (b) Silver content of alginate-AgNPs fibers synthesized at different temperature.

3.2. FE-SEM and EDS analysis of alginate-AgNPs fibers

In addition to the apparent change in the color of the fibers, which could be seen by the naked eyes, surface morphology and fine structures of the samples were subjected to further analysis by FE-SEM. Fig. 2 (a) show FE-SEM images of the pure alginate fibers prepared by wet spinning technique. It can be seen the prepared fibers present homogenous and smooth surface without particle deposition. Compared to the pure alginate fibers shown in Fig. 2(a), the morphology of alginate-AgNPs fibers has no observable change [Fig. 2(b) and (c)]. However, the surfaces of fibers are rough and uneven, AgNPs coated on the fiber surface are clearly observed by higher magnification [the inset Figures of Fig. 2(b) and (c)] and exhibit homogeneous distribution in nano-meter scale. Additionally, the coverage density of AgNPs on the surface of alginate-AgNPs fibers prepared at 80 °C appears to be less than that of the fibers prepared at 60 °C. The reason might be that silver ions diffused more rapidly inside the fibers at higher temperature. [3]

EDS is a widely utilized tool to provide qualitative and quantitative information of elements that may be involved in the formation of AgNPs where the X-rays are generated in a region about 2 µm in depth.[31] The presence of AgNPs on the fibers was confirmed by EDS spectrum. As shown in Fig. 2(d), the peaks at around 3 kev are clearly seen and assigned to the silver signal.[32, 33] EDS quantitative elemental analysis was also performed to investigate the bulk atomic composition of the major elements in the alginate-AgNPs fibers (Table S1). The content of Ag is 4.35 wt%, higher than the data from ICP-OES (2.03 wt %), suggesting that more AgNPs distributed on surface of the fibers than that inside of the fibers.

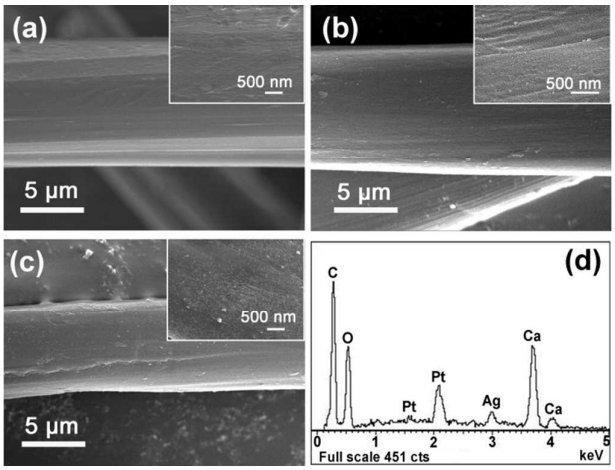

Fig. 2 FE-SEM micrographs of (a) Pure alginate fibers, (b) alginate-AgNPs fibers synthesized at 60 °C, 12 mM $AgNO_3$, (c) alginate-AgNPs fibers synthesized at 80 °C, (d) EDS spectrum of alginate-AgNPs fibers synthesized at 80 °C, 12mM $AgNO_3$.

3.3. TEM and XRD analysis of alginate-AgNPs fibers

Fig. 3 presents the typical TEM images of alginate-AgNPs fibers in cross sections. From the TEM images, it can be seen clearly that dispersed AgNPs have been generated in situ, which are embedded into alginate fibers. The small black AgNPs are not only located on the surface but also the inside of the fibers. Moreover, no aggregation are observed in Fig. 3. This indicates that the formed AgNPs can be effectively

stabilized by the alginate fibers. AgNPs might interact with the alginate matrix mainly by van der Waals interactions.[34] In this process, the alginate fibers played an important role as stabilizers for the formation of AgNPs and prevented AgNPs from agglomeration and aggregation. Apparently, nucleation in the alginate fibers was fostered, while the subsequent growth of supercritical particles was limited by the restricted diffusion of Ag^+ in the alginate fibers during the synthesis of the particles. Hence, the present process to generate AgNPs supported in alginate fibers involved in a controlled nucleation and a limited growth of AgNPs which did not aggregate and coalescence.[22] Additionally, the distribution of AgNPs is graded from the surface toward the center in the fibers. Interestingly, when the reaction temperature was increased, the number of the AgNPs on the fiber surface decreased, while increased inside the fiber, this might be attributed to the enhanced mobility of Ag ions at higher temperature. This would reduce the quantity of Ag ions on the fiber surface and, correspondingly, the yield of AgNPs. These results are consistent with the SEM results. Particle size distribution histograms of AgNPs in the fibers [the inset of Fig. 3 (c) and (f)] illustrate that the particle size seem to be in the range of 10-25nm. The particle size marginally increases with the increase of reaction temperature.

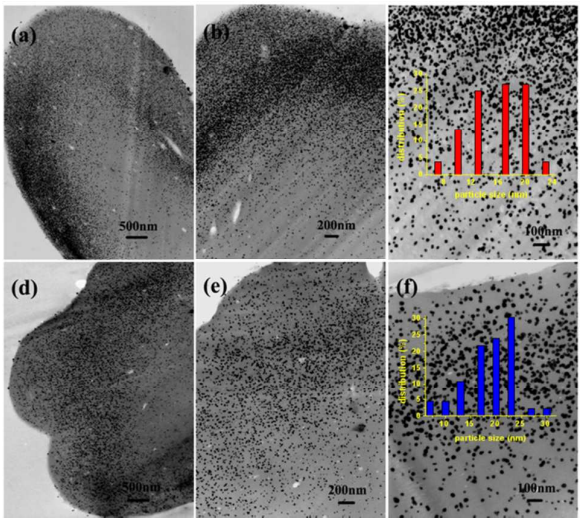

Fig. 3 TEM images of alginate-AgNPs fibers in cross sections. (a) (b) (c) alginate-AgNPs fibers synthesized at 60 °C, 12 mM $AgNO_3$ with different magnification, (d) (e) (f) alginate-AgNPs fibers synthesized at 80 °C, 12 mM $AgNO_3$. The insets in Fig. 5(c) and (f) show the particle size distribution of AgNPs in the fibers.

The crystalline natures of the alginate-AgNPs fibers were also confirmed by analysis of the XRD pattern. Fig. 4 shows the XRD patterns of pure alginate fiber and alginate-AgNPs fibers. It can be seen that the pure alginate fiber do not reveal any diffraction peak for silver, while alginate-AgNPs fibers reveal distinct diffraction peaks at 2θ=38.2°, 44.4°, 64.3°, and 77.2°, which are attributed to (111), (200), (220), and (311) crystal planes of silver, respectively. These typical XRD peaks indicate the formation of a face centred cubic (fcc) structure of the crystalline AgNPs in alginate fibers. Among the corresponding planes, (111) plane exhibits a higher intensity than the other planes, suggesting that the (111) plane is the predominant orientation.[35] The intensity of the diffraction peaks varies with increasing concentration of the $AgNO_3$ and reaction temperature. The single diffraction peak (111) can be observed in Fig. 4 (b), which might be due to the low content of AgNPs in alginate fibers.

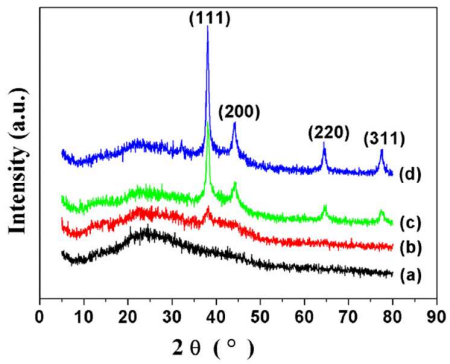

Fig. 4 XRD patterns of alginate firbes with silver nanoparticles. (a) Pure alginate fibers; (b) alginate-AgNPs fibers synthesized (60 °C, 12 mM $AgNO_3$); (c) alginate-AgNPs fibers synthesized (80 °C, 12 mM $AgNO_3$); (d) alginate-AgNPs fibers synthesized (60 °C, 24 mM $AgNO_3$).

3.4. XPS analysis of alginate-AgNPs fibers

X-ray photoelectron spectroscopy (XPS) is often used in the surface analysis of the materials, due to its high surface sensitivity and chemical specificity in the identification of the elements on the surfaces, concomitantly with their chemical valence. Fig. S1(a) shows survey XPS patterns of alginate-AgNPs fibers . The XPS analysis shows the presence of oxygen, carbon, silver and calcium in the fibers. The deconvolution of the XPS core-level spectrum in the region characteristic to silver species appears two obvious peaks of Ag 3d fundamental bands at the binding energy of 368.0 (3d5/2) and 374.3 eV (3d3/2), [Fig. S1(b)], which mainly attributes to Ag^0 configuration.[36]

3.5. Catalytic activity of alginate- AgNPs fibers

In this study, the reduction of 4-NP to 4-AP by $NaBH_4$ was chosen as a model system to quantitatively evaluate the catalytic activity of the as-prepared alginate-AgNPs fibers. Although, it has been well documented that this reaction is a thermodynamically feasible process involving standard reduction potential for 4-NP/4-AP = —0.76 and H_3BO_3/BH_4^- = —1.33 V versus a normal hydrogen electrode, it is kinetically restricted in the absence of a catalyst. [3, 37]

Normally, the absorption peak of 4-nitrophenol undergoes a red shift from 317 to 400 nm immediately upon addition of the $NaBH_4$ solution, corresponding to a significant change in solution color from light yellow to yellow-green,

which is due to the generation of 4-nitrophenolate ion at the alkaline conditions (Fig. 5(a) and (b)). In the absence of catalyst, the absorption peak at 400 nm stayed unchanged in intensity for a long duration, indicating 4-NP is not reduced effectively by $NaBH_4$ or the reduction rate is very slow. In contrast, after adding alginate-AgNPs fibers into the reaction medium, the absorption peak of 4-NP at 400 nm gradually decreased along with the appearance of a new absorption peak of 4-AP at 300 nm (Fig. 5(c)), suggesting the successful reduction of 4-NP to 4-AP. The reason is that, as suggested by Zhang et al.[27, 38], the catalyst brings down the kinetic barrier created due to mutual repulsion between negatively charged 4-nitrophenolate ion and BH_4^- ion. The silver nanoparticles provoke the catalytic reduction by relaying electrons from the donor BH_4^- to the acceptor 4-NP through adsorption of the reactant molecules onto the surfaces of the catalyst (Fig. 6), where the alginate-AgNPs fibers accepts electrons from BH_4^- ions and conveys them to 4-NP. At the early stage, BH_4^-could be adsorbed and reacted with the surface of as-prepared alginate-AgNPs fibers, thereby, a surface-hydrogen species could be formed and transferred to the surface of AgNPs to form the metal hydride [Step (1)].[9,39] 4-NP could also easily transport to the AgNPs surface because of the strong adsorption of alginate-AgNPs fibers [Step (2)]. These two steps are reversible, moreover, the diffusion of both reactants to alginate-AgNPs fibers and adsorption/desorption equilibriums of these reactants on the surface are very fast. Then, the reduction of 4-NP was provoked by the interaction of the adsorbed 4-NP with the Ag nanoparticles surface-bound hydrides.[9], 4-AP formed as a result of reduction reaction [Step (3)]. When the formed 4-AP desorbed from the AgNPs surfaces, the next new catalytic reduction cycle can be proceeded again [Step (4)]. It should be noted that the H_2 generated, during this process, is beneficial to remove the 4-AP from the AgNPs surfaces, thus keeping the surface fresh and maintaining the high reactivity of the nanoparticles.[40, 41]

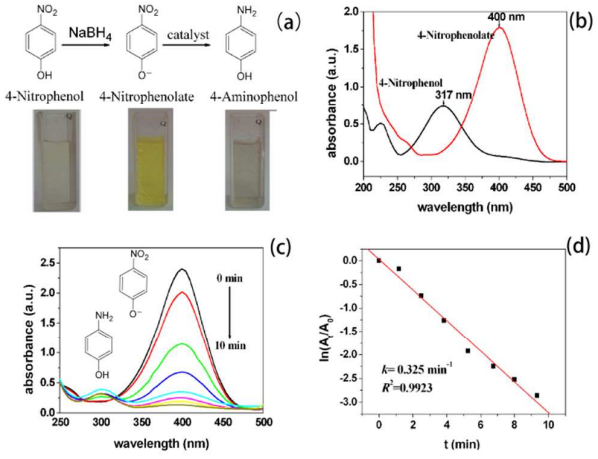

Fig. 5 The reduction reaction for the conversion of 4-NP to 4-AP (a); UV-vis absorption spectra of 4-NP before and after addition of $NaBH_4$ (b); the successive reduction of 4-NP to 4-AP over alginate-AgNPs fibers (synthesized at 60 °C, 24 Mm $AgNO_3$) catalyst (c); Plot of $\ln(A_t/A_0)$ against the reaction time (d).

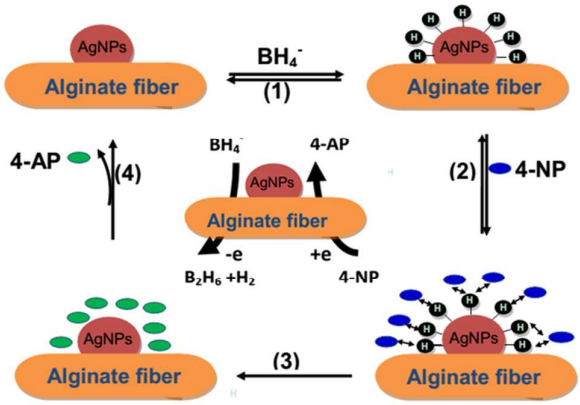

Fig. 6 The proposed mechanism of the reduction of the 4-NP by $NaBH_4$ in the presence of alginate-AgNPs fibers.

In the reaction medium, the amount of $NaBH_4$ is in excess compared to 4-NP, which remains essentially constant during the reaction. Hence, the pseudo-first-order reaction would be reasonable assumption to evaluate the performance of the catalysts.[37] Since the absorbance is proportional to the concentration of 4-NP, the ratio of the concentration of 4-NP at time t to that at time 0 (C_t/C_0) must be equal to the ratio of the absorbance at time t to that at time 0 (A_t/A_0). Therefore, the kinetic process for the reduction of 4-NP can be easily studied by simply monitoring the change in the absorbance at 400 nm. The plots of $\ln(A_t/A_0)$ versus reaction time for the reduction of 4-NP by $NaBH_4$ over alginate-AgNPs fibers as catalysts are displayed in Fig. 5(d). A good linear correlation of $\ln(A_t/A_0)$ versus time was obtained and a kinetic reaction rate constant k was estimated to be 0.325 min^{-1} by fitting the curves.

The catalytic activities of varied formed alginate-AgNPs fibers were compared in the reaction of 4-NP reduction (Fig. S2). It can be seen the catalytic action cloud be completed with 15 min in all case. The plots of $\ln(A_t/A_0)$ versus time with varied formed alginate-AgNPs fibers are demonstrated in Fig. S3. Obviously, all curves displayed the first-order kinetics (All R^2 of the fitted lines are more than 0.98). The corresponding rate constants k are 0.430 min^{-1}, 0.490 min^{-1} and 0.363 min^{-1} respectively as alginate-AgNPs fibers formed at 80 °C for 45 min with silver nitrate concentration of 8 mM, 16 mM and 24 mM accordingly (Fig. S3(a)). The k were 0.240 min^{-1}, 0.315 min^{-1}, 0.346 min^{-1} as alginate-AgNPs fibers synthesized at 60 °C,70 °C and 80 °C for 45 min with silver nitrate concentration of 12 mM, respectively (Fig. S3(b)). As the previous study, k was well related with the total surface area of AgNPs in the fibers which depended on the size, distribution and content of AgNPs in the fibers.[42] Smaller particle size or much more AgNPs in the fibers will increase

the catalytic activity. Much more AgNPs formed in the fibers at higher $AgNO_3$ concentration and reaction temperature will increase the catalytic activity, but, the increasing particle size will decrease the catalytic activity.

The reusability and the catalytic stability is the important factor for practical applications of the catalyst. The recyclability of the as-prepared alginate-AgNPs fibers (the representative sample formed at 80 ^{o}C for 45 min with silver nitrate concentration of 16 mM) was investigated by monitoring catalytic activity during successive cycles of the reduction reaction. The activity is calculated based on the reduction of the reaction rate relative initial rate for each use. After the completion of the reduction reactions of 4-NP, the used fibers were washed with water for the next catalytic run. As shown in Fig. 7, alginate-AgNPs fibers were reused for ten cycles for the reduction reaction of 4-NP with a conversion efficiency more than 97%, indicating the excellent stability of the obtained catalysts, this could be attribute to alginate fibers preventing the immobilized AgNPs from aggregating. From TEM image of recycled fiber sample (Fig. S4), we also can observe that AgNPs are well dispersed in alginate fibers without remarkable aggregation, further confirming the stabilization effect of alginate fibers to AgNPs. Additionally, the activity reduced to about 90% after ten cycles, this may be due to the poisoning of AgNPs from the coverage of 4-AP on the surface of the catalysts or catalyst inactivation. [6] All these results indicated that alginate-AgNPs fibers are excellent catalysts with superior stability and recyclability for the reduction of 4-NP, which endow the possibility of their practical applications.

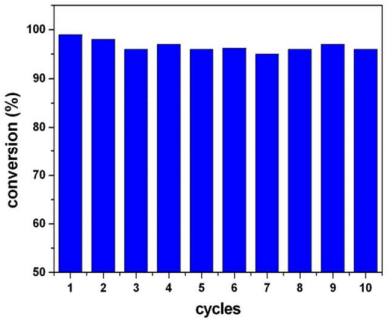

Fig. 7 Recyclability test result of alginate-AgNPs fibers by ten runs of repeated usage.

4. Conclusions

Alginate-AgNPs fibers were successfully prepared *via* in situ reduction of Ag^{+}-alginate fibers. Spherical AgNPs could be effectively dispersed and stabilized in the surface and interior of alginate fibers with diameter 10-25 nm. The distribution of AgNPs was graded from the outside toward the center in the fibers. The alginate-AgNPs fibers showed excellent catalytic activity for the reduction of 4-NP in the presence of $NaBH_4$. The catalytic stability was also superior with the conversion remaining over 95% after ten cycles of catalytic reaction. The easy accessibility, high performance catalyst may strongly encourage the practical applications of 4-NP reduction. This facile method is also potentially expanded to the preparation of other alginate-metal nanoparticles composite materials.

Acknowledgements

This work is supported by the Natural Science Foundation of China (No. 51203083), Special Fund for Self-directed Innovation of Shandong Province of China (No. 2013CXB80201) and the Key Technologies R&D Program of Qingdao (No. 12-4-1-48-hy).

Notes and references

1. S. Saha, A. Pal, S. Kundu, S. Basu and T. Pal, *Langmuir*, 2010, **26**, 2885-2893.
2. L. Ai, H. Yue and J. Jiang, *J. Mater. Chem.*, 2012, **22**, 23447-23453.
3. Z. Xu and G. Hu, *RSC Adv.*, 2012, **2**, 11404–11409.
4. Y. Zheng and A. Wang, *J. Mater. Chem.*, 2012, **22**, 16552-16559.
5. S. Naraginti and A. Sivakumar, *Spectrochim. Acta A*, 2014, **128**, 357-362.
6. Z. Dong, X. Le, X. Li, W. Zhang, C. Dong and J. Ma, *Appl. Catal. B-Environ.*, 2014, **158**, 129-135.
7. M. B. Gawande,S. N. Shelke, R. Zboril,and R. S. Varma, *Acc. Chem. Res.*, 2014, **47**, 1338-1348.
8. C. Levard, E. M. Hotze, G. V. Lowry, and G. E. Brown, Jr., *Environ. Sci. Technol.*, 2012, **46**, 6900-6914.
9. H. -L. Lin, N. -L. Sou and G. G. Huang, *RSC Adv.*, 2015, **5**, 19248-19254.
10. X. Lv, Y. Zhu, H. Jiang, H. Zhong, X. Yang and C. Li, *Dalton T.*, 2014, **43**, 15111-15118.
11. M. N. Nadagouda, T. F. Speth, and R. S. Varma, *Acc. Chem. Res.*, 2011, **44**, 469-478.
12. C. J. Li and L. Chen, *Chem. Soc. Rev.*, 2006, **35**, 68-82.
13. M. Horecha, E. Kaul, A. Horechyy and M. Stamm, *J. Mater. Chem. A*, 2014, **2**, 7431-7438.
14. J. Gao, J. Xu, S. Wen, J. Hu and H. Liu, *Micropor. Mesopor. Mat.*, 2015, **207**, 149-155.
15. A. Bilici, B. Ayten and I. Kaya, *Synthetic Met.*, 2015, **201**, 11-17.
16. Z. Jiang, D. Jiang, A. M. S. Hossain, K. Qian and J. Xie, *Phys. Chem. Chem. Phys.*, 2015, **17**, 2550-2559.
17. X. Le, Z. Dong, Y. Liu, Z. Jin, H. Thanh-Do, L. Minhdong and J. Ma, *J. Mater. Chem. A*, 2014, **2**, 19696-19706.
18. T. Benko, A. Beck, K. Frey, D. F. Sranko, O. Geszti, G. Safran, B. Maroti and Z. Schay, *Appl. Catal. A-Gen.*, 2014, **479**, 103-111.
19. Y. Zheng, Y. Zhu, G. Tian and A. Wang, *Int. J. Biol. Macromol.*, 2015, **73**, 39-44.
20. Q. Geng and J. Du, *RSC Adv.*, 2014, **4**, 16425-16428.
21. M. B. Gawande, V. D. B. Bonifacio, R. Luque, P. S. Branco and R. S. Varma, *Chem. Soc. Rev.*, 2013, **42**, 5522-5551.
22. Y. Lu, Y. Mei, M. Schrinner, M. Ballauff and M. W. Moeller,

J. Phys. Chem. C, 2007, **111**, 7676-7681.
23. J. Wu, N. Zhao, X. Zhang and J. Xu, *Cellulose*, 2012, **19**, 1239-1249.
24. Y. Qin, *Polym. Int.*, 2008, **57**, 171-180.
25. P. Sikorski, F. Mo, G. Skjak-Braek and B. T. Stokke, *Biomacromolecules*, 2007, **8**, 2098-2103.
26. L. Li, Y. Fang, R. Vreeker and I. Appelqvist, *Biomacromolecules*, 2007, **8**, 464-468.
27. H. Hu, J. H. Xin and H. Hu, *J. Mater. Chem. A*, 2014, **2**, 11319-11333.
28. Y. Li, Y. Cao, J. Xie, D. Jia, H. Qin and Z. Liang, *Catal. Commun.*, 2015, **58**, 21-25.
29. A. M. Abdel-Mohsen, R. Hrdina, L. Burgert, G. Krylova, R. M. Abdel-Rahman, A. Krejcova, M. Steinhart and L. Benes, *Carbohyd. Polym.*, 2012, **89**, 411-422.
30. M. Radetic, *J. Mater. Sci.*, 2013, **48**, 95-107.
31. R. M. El-Shishtawy, A. M. Asiri, N. A. M. Abdelwahed and M. M. Al-Otaibi, *Cellulose*, 2011, **18**, 75-82.
32. J. Y. Song and B. S. Kim, *Bioproc. Biosyst. Eng.*, 2009, **32**, 79-84.
33. F. M. Reicha, A. Sarhan, M. I. Abdel-Hamid and I. M. El-Sherbiny, *Carbohyd. Polym.*, 2012, **89**, 236-244.
34. S. Lin, R. Huang, Y. Cheng, J. Liu, B. L. T. Lau and M. R. Wiesner, *Water Res.*, 2013, **47**, 3959-3965.
35. P. Kanmani and J.-W. Rhim, *Food Chem.*, 2014, **148**, 162-169.
36. A. Chibac, V. Melinte, T. Buruiana, L. Balan and E. C. Buruiana, *Chem. Eng. J.*, 2012, **200**, 577-588.
37. B. J. Borah and P. Bharali, *J. Mol. Catal. a-Chem.*, 2014, **390**, 29-36.
38. J. Zhang, L. Li, X. Huang and G. Li, *J. Mater. Chem.*, 2012, **22**, 10480-10487.
39. X.-Q. Wu, X.-W. Wu, Q. Huang, J.-S. Shen and H.-W. Zhang, *Appl. Surf. Sci.*, 2015, **331**, 210-218.
40. S. Wunder, F. Polzer, Y. Lu, Y. Mei and M. allauff, *J. Phys. Chem. C*, 2010, **114**, 8814-8820.
41. B.H. Liu, and Z.P. Li, *J. Power Sources*, 2009, **187**, 527-534.
42. W. Xu, W. Jin, L. Lin, C. Zhang, Z. Li, Y. Li, R. Song and B. Li, *Carbohyd. Polym.*, 2014, **101**, 961-967.

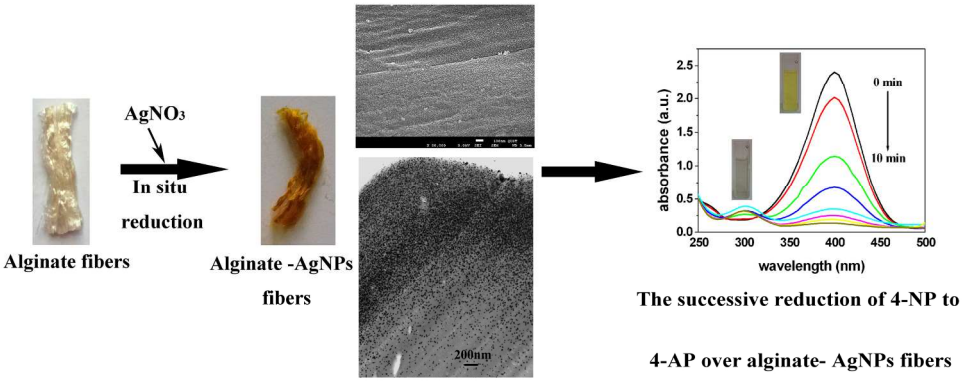

207x84mm (300 x 300 DPI)